

Real-Time Reliable Prediction of Linear-Elastic Mode-I Stress Intensity Factors for Failure Analysis

D.B.P. HUYNH¹, J. PERAIRE^{1,3}, A.T. PATERA^{1,3} and G.R. LIU^{1,2}

¹Singapore-MIT Alliance

²National University of Singapore

³Massachusetts Institute of Technology

Abstract—Modern engineering analysis requires accurate, reliable and efficient evaluation of outputs of interest. These outputs are functions of “input” parameter that serve to describe a particular configuration of the system, typical input geometry, material properties, or boundary conditions and loads. In many cases, the input-output relationship is a functional of the field variable - which is the solution to an input-parametrized partial differential equations (PDE). The reduced-basis approximation, adopting off-line/on-line computational procedures, allows us to compute accurate and reliable functional outputs of PDEs with rigorous error estimations. The operation count for the on-line stage depends only on a small number N and the parametric complexity of the problem, which make the reduced-basis approximation especially suitable for complex analysis such as optimizations and designs. In this work we focus on the development of finite-element and reduced-basis methodology for the accurate, fast, and reliable prediction of the stress intensity factors or strain-energy release rate of a mode-I linear elastic fracture problem. With the use of off-line/on-line computational strategy, the stress intensity factor for a particular problem can be obtained in milliseconds. The method opens a new promising prospect: not only are the numerical results obtained only in milliseconds with great savings in computational time; the results are also reliable - thanks to the rigorous and sharp a posteriori error bounds. The practical uses of our prediction are presented through several example problems.

Index Terms—reduced-basis approximation, a posteriori error estimation, linear elasticity, stress intensity factor, brittle failure

I. INTRODUCTION

Fracture Mechanics [6] provides the theory of failure analysis of material and structures containing cracks; the stress intensity factor (SIF) is a key quantity because it indicates the singular intensity of linear elastic crack field. SIF plays a dominant role in many fracture mechanics applications such as fatigue crack growth prediction or analysis of ultimate crack instability and failure.

However, exact solution of the SIF can be obtained for just a few problems, even in such cases, SIF data are usually presented in either tabular form or graphic diagrams [9], which make it difficult to extract the information accurately by either correlations or interpolations. For complicated problems, SIF solutions are sought by numerical methods such as finite element method and boundary element method, which are usually very expensive [12]. Hence current SIF procedures are either fast but not necessarily reliable – the former – or reliable but not very fast – the latter. Because practical applications usually involve a real-time context (such as non-destruction evaluation (NDE) or online safely monitoring) or

a many-query context (such as robust sensitivity/uncertainty analysis or fatigue analysis), current SIF procedures are often adequate.

We present in this paper a technique for the rapid and reliable prediction of the SIF outputs of a crack model with parameter dependence. The essential ingredients are (i) rapidly convergent reduced-basis approximations that provide inexpensive solution by Galerkin projection onto a space W_N spanned by solutions of the governing partial differential equation (PDE) at N selected points in parameter space; (ii) a posteriori error estimation that provides inexpensive yet sharp bounds for the error in the output of interest; and (iii) offline/online computational procedures – method that decouple the generation and projection stages of the approximation process – which allow us to calculate the output of interest and associated error bound in very few operations (depending only on N , typically small).

This paper is organized as follows. In the next section we will present the formulation of our linear-elastic Mode-I fracture problem. The reduced-basis approximation and our a posteriori error estimation is discussed in Section III and Section IV, respectively. Several fracture mechanics applications are given in Section V. Finally, Section VI provides some brief concluding remarks.

II. MODEL PROBLEM

A. Problem description

We consider a linear elasticity problem corresponding to a crack notch inside a two-layer materials plate. The left material may be viewed as a coating providing protection. We show in Figure 1 the original domain of the problem, $\Omega^0(d)$, consisting of two layers Ω_1^0 and Ω_2^0 corresponds to two different materials with Young modulus \bar{E}_1 and \bar{E}_2 , respectively and the same Poisson’s ratio $\nu_1 = \nu_2 = \nu$. The two layers Ω_1^0 and Ω_2^0 are of width \tilde{t} and $4\tilde{t}$, respectively. The crack is of length \tilde{d} , the plate is of length $\tilde{w} \equiv 5\tilde{t}$ and of height $4\tilde{w}$. We impose traction $\tilde{\sigma}_0$ at the top Γ_T , Neumann symmetry condition of the plate centerline Γ_C , and Dirichlet boundary condition on the right side of the plate Γ_R . The displacement field $\tilde{u}^e(\tilde{x}^e; \mu)$ satisfies the (plain strain) linear elasticity equation in Ω^0 . Using non-dimensional terms,

$$E_{1,2} \equiv \frac{\bar{E}_{1,2}}{1-\nu^2} \quad x \equiv \frac{\tilde{x}}{\tilde{t}} \quad d \equiv \frac{\tilde{d}}{\tilde{t}} \quad u \equiv \frac{\tilde{u}\bar{E}_1}{\tilde{\sigma}_0\tilde{t}}, \quad (1)$$

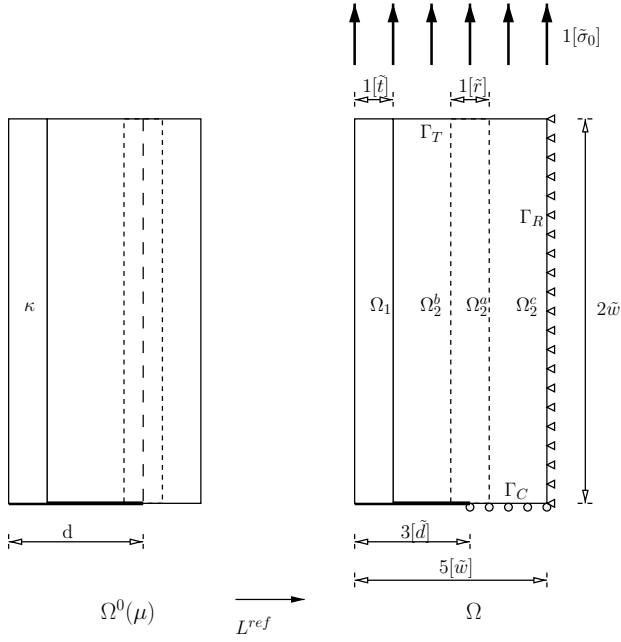


Fig. 1. Fracture problem: (a) Reference domain, and (b) Original domain

we can write the non-dimensional governing equation for the displacement field $u^e(x^e; \mu) \in X^e(\mu)$ as

$$a(u^e, v; \mu) = f(v; \mu), \forall v \in X^e \quad (2)$$

where X^e is the appropriate Hilbert space defined over the physical domain Ω^0 , and a and f are continuous bilinear and linear forms given by

$$a(u^e, v; \mu) = \int_{\Omega_1} \frac{\partial u_i^e}{\partial x_j} E_{ijkl}^{(1)} \frac{\partial v_k}{\partial x_l} + \int_{\Omega_2} \frac{\partial u_i^e}{\partial x_j} E_{ijkl}^{(2)} \frac{\partial v_k}{\partial x_l} \quad (3)$$

$$f(v; \mu) = \int_{\Gamma_a} v. \quad (4)$$

In our plain-strain assumption, $E_{ijkl}^{(1,2)} = \tilde{c}_1^{(m)} \delta_{ij} \delta_{kl} + \tilde{c}_2^{(m)} (\delta_{ik} \delta_{jl} + \delta_{il} \delta_{jk})$ is the constitutive tensor, where $\tilde{c}_1^{(1,2)}$ and $\tilde{c}_2^{(1,2)}$ are Lamé's constants, related to Poisson's ration, ν , and the ratio of the two non-dimensional Young modulus, $\kappa = \tilde{E}_1 / \tilde{E}_2$, by

$$\tilde{c}_1^{(1)} = \frac{\kappa \nu}{(1 + \nu)(1 - 2\nu)}, \quad \tilde{c}_2^{(1)} = \frac{\kappa}{2(1 + \nu)} \quad (5)$$

$$\tilde{c}_1^{(2)} = \frac{\nu}{(1 + \nu)(1 - 2\nu)}, \quad \tilde{c}_2^{(2)} = \frac{1}{2(1 + \nu)}. \quad (6)$$

We shall consider $P = 2$ parameters, $\mu_1 \equiv d$ (non-dimensional length of the crack) and $\mu_2 \equiv \kappa$ (ratio of the two non-dimensional Young modulus), for the parameter domain $\mathcal{D} = [2.0, 4.0] \times [0.1, 10]$.

In order to apply our methodology we map $\Omega^0(d) \rightarrow \tilde{\Omega} \equiv \Omega^0(d = d^{\text{ref}} = 3)$. The domain Ω_2 is further divided into three domains Ω_2^a , Ω_2^b and Ω_2^c . The transformation is piecewise affine: an identity for Ω_1 , Ω_2^b ; and dilations for Ω_2^a and Ω_2^c . In these mapped coordinates, $a(u^e, v; \mu)$ and $f(v; \mu)$ can be

expressed as

$$a(u^e, v; \mu) = \sum_{q=1}^{Q_a} \Theta_a^q(\mu) a^q(u^e, v) \quad (7)$$

$$f(v; \mu) = \sum_{q=1}^{Q_f} \Theta_f^q(\mu) f^q(v), \quad (8)$$

where $Q_a = 6$, $Q_f = 3$.

B. Output definitions

The methods for extracting SIF from a finite element solution fall into two categories: displacement matching methods (such as the displacement correlation technique [7]) and energy based methods (including the J-integral approach [8] and the virtual crack extension approach [10]). In the former category, the displacement values of nodes near the crack are used to extract the coefficients of the asymptotic expansion, assumed that the form of the local solution is already known. In the latter category, SIF is related directly to the energy release rate (ERR).

The displacement matching methods have some advantages over the energy based methods, such that they are usually much simpler and easier to derive, but they have some drawbacks as well. One of the major disadvantages of these methods is that the form of the output functional is usually unbounded, thus leading to difficult theoretical and numerical questions. The energy based method, in the other hand, usually provide bounded output functional form, so the convergence is at least guaranteed. There are a number of energy-based approaches to compute the ERR; for example, Parks [10] used matrix stiffness derivatives to compute ERR by taking note that the contribution to ERR is only from elements near crack-tip region. In this paper, we will directly compute the ERR by taking advantage of our parametrized form.

For Mode-I fracture problems, the SIF K can in fact be extracted directly from the ERR. ERR is defined by $G^e = -\frac{\partial \Pi^e}{\partial d}$, where Π^e is the total potential energy; the total potential energy of our finite element model is given by $\Pi^e(\mu) = \frac{1}{2} a(u^e(\mu), u^e(\mu); \mu) - f(u^e(\mu); \mu)$. We can write (non-dimensional) G and (dimensional) K as

$$G\left(\frac{\tilde{d}}{\tilde{t}}, \frac{\tilde{E}_2}{\tilde{E}_1}\right) = -\frac{1}{2} \frac{\partial}{\partial d} a(\cdot, \cdot; \mu) + \frac{\partial}{\partial d} f(\cdot; \mu) \quad (9)$$

$$\tilde{K}(\tilde{\sigma}_0, \tilde{d}, \tilde{t}, \tilde{E}_1, \tilde{E}_2) = \tilde{\sigma}_0 \sqrt{\tilde{t}} \sqrt{G\left(\frac{\tilde{d}}{\tilde{t}}, \frac{\tilde{E}_2}{\tilde{E}_1}\right)}, \quad (10)$$

respectively. Note that $\frac{\partial}{\partial d}$ is the differentiation with respect to only d .

We define our output of interest $s^e(\mu) = G^e(\mu)$, and hence

$$s^e(\mu) = s_1^e(\mu) + s_2^e(\mu) \quad (11)$$

where

$$s_1^e(\mu) = l(u^e(\mu), \mu) \quad (12)$$

$$s_2^e(\mu) = p(u^e(\mu), u^e(\mu), \mu), \quad (13)$$

where l and p are continuous (bounded) linear and bilinear

forms defined by

$$l(\cdot; \mu) = \frac{\partial}{\partial d} f(\cdot; \mu) \quad (14)$$

$$p(\cdot, \cdot; \mu) = -\frac{1}{2} \frac{\partial}{\partial d} a(\cdot, \cdot; \mu). \quad (15)$$

Our (output) bilinear and linear form are also affine in the parameters

$$l(v; \mu) = \sum_{q=2}^{Q_f} \left[\frac{\partial \Theta_f^q(\mu)}{\partial a} \right] f^q(v) \quad (16)$$

$$\begin{aligned} p(w; v; \mu) &= \sum_{q=3}^{Q_a} \left[-\frac{\partial \Theta_a^q(\mu)}{\partial a} \right] a^q(w, v) \\ &= \sum_{q=1}^{Q_p} \Theta_p^q(\mu) p^q(w, v), \end{aligned} \quad (17)$$

where $w, v \in X^e$. We note that $\frac{\partial \Theta_a^q}{\partial a} = 0$ for $q = 1, 2$ so $Q_p = Q_a - 2$.

C. Finite element formulation

The singular crack-tip stress and strain fields cause a very difficult problem for solving fracture mechanics problem by finite element method. The polynomial basis spaces used for most conventional elements cannot capture these behaviours, and thus the finite element solution converges very slowly to the theoretical solution when the mesh is refined. To overcome this difficulty, various attempts have been made to include these singularities in the element formulation. The two most common treatments for this difficulty are the ‘‘quarter-point’’ element suggested by Barsoum [2] and Shaw [5], or the enriched finite element method [12] and more recent generalization [3].

The ‘‘quarter-point’’ element captures the singularity of the stress and strain fields by moving the element’s mid-side node to the position one quarter of the way from the crack tip to the far end of the element. Although it is accurate and easy to use, the crack tip field is not reproduce exactly, and the method does not have a firm theoretical ground.

The enriched finite element method exploits the partition of unity property of finite elements identified by Melenk and Babuska [1] which allows local enrichment functions to be incorporated into a finite element approximation. For fracture mechanics problems, the region around the crack-tip is enriched by the the local function of the asymptotic fields, and thus can capture the singularity of the fields exactly if correct enriched functions are used.

We define our finite element approximation space as

$$X^{\mathcal{N}} = X_1 \times X_2, \quad (18)$$

where $u \equiv (u_1, u_2) \in X^{\mathcal{N}}$, and

$$\begin{aligned} X_1 &= X_{1h,p} + \text{span}\{\Upsilon \Psi_{j,1 \leq j \leq 4}\} \\ X_2 &= X_{2h,p} + \text{span}\{\Upsilon \Psi_{j,1 \leq j \leq 4}\}, \end{aligned} \quad (19)$$

where $X_{(\frac{1}{2})h,p}$ is our usual p^{th} order finite element space, Υ is the partition of unity function valid in a small ‘‘enriched’’

region around the crack tip, and Ψ_j is the enriched function defined based on the asymptotic fields. For homogeneous material around the crack [3],

$$\Psi_j(r, \theta) = \left\{ \sqrt{r} \sin \frac{\theta}{2}, \sqrt{r} \cos \frac{\theta}{2}, \sqrt{r} \sin \frac{\theta}{2} \sin \theta, \sqrt{r} \cos \frac{\theta}{2} \sin \theta \right\}, \quad (20)$$

where (r, θ) are the local polar co-ordinates at the crack tip.

In general, we cannot find the exact solution for (2), hence we replace $s^e(\mu), u^e(\mu)$ with a Galerkin finite element approximation, $s(\mu) \equiv s^{\mathcal{N}_t}, u(\mu) \equiv u^{\mathcal{N}_t}$: given $\mu \in \mathcal{D}$,

$$a(u(\mu), v; \mu) = f(v), \forall v \in X^{\mathcal{N}_t} \equiv X \quad (21)$$

and

$$s(\mu) = s_1(\mu) + s_2(\mu), \quad (22)$$

where

$$s_1(\mu) = l(u(\mu); \mu), s_2(\mu) = p(u(\mu), u(\mu); \mu), \forall v \in X. \quad (23)$$

Here $X \subset X^e$ is our finite element approximation subspace of dimension \mathcal{N} defined above. We assume that \mathcal{N} is large enough so our approximate solution is near to the ‘‘truth’’ solution. Note our online complexity will be independent of \mathcal{N} .

We denote the inner product and norm associated with our Hilbert space $X (\equiv X^{\mathcal{N}_t})$ as $(w, w)_X$ and $\|v\|_X = \sqrt{(v, v)_X}$, respectively. We further define the dual norm for any bounded linear functional h as

$$\|h\|'_X \equiv \sup_{v \in X} \frac{h(v)}{\|v\|_X}; \quad (24)$$

In our case, we may choose

$$(w, v)_X = \int_{\Omega} \frac{\partial w_i}{\partial x_j} E_{ijkl} \frac{\partial v_k}{\partial x_l}. \quad (25)$$

We next introduce the linear operator $T^\mu : X \rightarrow X$ such that,

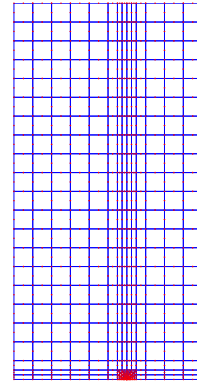


Fig. 2. Finite element mesh

for any w in X ,

$$(T^\mu w, v)_X = a(w, v; \mu), \forall v \in X. \quad (26)$$

We can then define a symmetric positive-semidefinite eigenvalue problem related to the (squared of the) singular values

of out partial differential operator: given $\mu \in \mathcal{D}$, $(\Phi_i(\mu))_i \in X$, $\rho_i(\mu) \in \mathbb{R}$, $i = 1, \dots, \mathcal{N}_t$, satisfies

$$(T^\mu \Phi_i(\mu), T^\mu v)_X = \rho_i(\mu) (\Phi_i(\mu), v)_X, \forall v \in X; \quad (27)$$

the eigenvalues are ordered such that $0 \leq \rho_1 \leq \rho_2 \leq \dots \leq \rho_{\mathcal{N}_t}$. We normalize our eigenfunctions as $\|\Phi_i(\mu)\|_X = 1$, $i = 1, \dots, \mathcal{N}_t$, and hence orthogonality reads

$$\begin{aligned} (T^\mu \Phi_i(\mu), T^\mu \Phi_j(\mu))_X &= \rho_i(\mu) (\Phi_i(\mu), \Phi_j(\mu))_X \\ &= \rho_i \delta_{ij}, 1 \leq i, j \leq \mathcal{N}_t, \end{aligned} \quad (28)$$

where δ_{ij} is the Kronecher-delta symbol. We may then identify $\beta^{\mathcal{N}_t}(\mu) \equiv \beta(\mu) = \sqrt{\rho_1(\mu)}$ and $\gamma^{\mathcal{N}_t}(\mu) \equiv \gamma(\mu) = \sqrt{\rho_{\mathcal{N}_t}(\mu)}$ where $\beta(\mu)$ is the continuity parameter

$$\beta(\mu) \equiv \inf_{w \in X} \sup_{v \in X} \frac{a(w, v; \mu)}{\|w\|_X \|v\|_X} \equiv \inf_{w \in X} \frac{\|T^\mu w\|_X}{\|w\|_X} \quad (29)$$

and $\gamma(\mu)$ is the usual continuity parameter,

$$\gamma(\mu) \equiv \sup_{w \in X} \sup_{v \in X} \frac{a(w, v; \mu)}{\|w\|_X \|v\|_X} \equiv \sup_{w \in X} \frac{\|T^\mu w\|_X}{\|w\|_X}. \quad (30)$$

For our problem, we observe that a is symmetric and coercive.

Our truth approximation space $X = X^{\mathcal{N}_t}$ is a (quadratic) finite element space of dimension $\mathcal{N} = \mathcal{N}_t = 2450$. The finite element mesh in Figure 2 is chosen as a mesh refined around the crack-tip to obtain better accuracy. The enrichment region is chosen as two nodal layers around the crack-tip.

We illustrate the convergence in term of $|\mathbf{E} - \mathbf{E}_h|/|\mathbf{E}_h|$ of our finite element model for the case $\mu = [3.0, 1.0]$ in Figure 3, where h is the average mesh length $h = \mathcal{N}^{-1/2}$ and \mathbf{E} denote our energy norm. The reference solution \mathbf{E}_h is chosen as the solution of a very fine mesh where $\mathcal{N}_h = 51845$. We note that the convergence of the model is improved relative to the classical FEM model as it correctly captures the singularity fields around the crack. The convergence rate of the model using linear elements is of order 2, which is equivalent to the analytical prediction. However, the convergence of the model using quadratic elements is only of order 3, which may be due to the fact that only the first singularity in the enrichment functions was used.

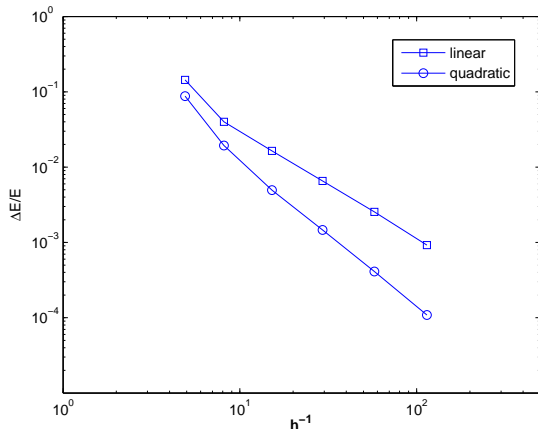


Fig. 3. Finite element convergence

III. REDUCED-BASIS APPROXIMATION

In this section, we shall build our reduced-basis approximation using the “truth” approximation and we shall evaluate the error in our reduced-basis approximation with respect to this “truth” approximation. We will only consider the quadratic output $s_2(\mu)$ in this section. The linear output $s_1(\mu)$, and the reduced-basis approximation (and its *a posteriori* error estimation) associated with it is discussed in details in [13].

A. Preliminary definitions

We first define $N = (N_{\text{pr}}, N_{\text{du}})$ where N_{pr} and N_{du} refer to the size of our primal and dual reduced-basis approximation spaces. We also specify $N_{\text{pr}, \text{max}}$ and $N_{\text{du}, \text{max}}$ as the upper limits on the dimensions of the primal and dual spaces, respectively.

We next introduce sets of primal and dual parameter points, $\mu_n^{\text{pr}}, 1 \leq n \leq N_{\text{pr}, \text{max}}$ and $\mu_n^{\text{du}}, 1 \leq n \leq N_{\text{du}, \text{max}}$, respectively. Our primal reduced-basis nested approximation spaces are then given by $W_{N_{\text{pr}}}^{\text{pr}} \equiv \text{span}\{u(\mu_n^{\text{pr}}), 1 \leq n \leq N_{\text{pr}}\}$, $1 \leq N_{\text{pr}} \leq N_{\text{pr}, \text{max}}$, where the $u(\mu_n^{\text{pr}}), 1 \leq n \leq N_{\text{pr}, \text{max}}$ are our “snapshot”. In actual practice we express $W_{N_{\text{pr}}}^{\text{pr}}$ in terms of the basis $\zeta_n^{\text{pr}}, 1 \leq n \leq N_{\text{pr}}$, where the $\zeta_n^{\text{pr}}, 1 \leq n \leq N_{\text{pr}, \text{max}}$, are generated from the $u(\mu_n^{\text{pr}}), 1 \leq n \leq N_{\text{pr}, \text{max}}$, by a Gram-Schmidt orthogonalization process relative to the $(\cdot, \cdot)_X$ inner product.

For given $\mu \in \mathcal{D}$, our primal approximation $u_{N_{\text{pr}}} \in W_{N_{\text{pr}}}^{\text{pr}}$ satisfies

$$a(u_{N_{\text{pr}}}, v; \mu) = f(v), \forall v \in W_{N_{\text{pr}}}^{\text{pr}}; \quad (31)$$

we denote the primal residual is

$$r_{N_{\text{pr}}}^{\text{pr}}(v; \mu) = f(v) - a(u_{N_{\text{pr}}}, v; \mu), \forall v \in X \quad (32)$$

and the primal error is $e^{\text{pr}}(\mu) = u(\mu) - u_{N_{\text{pr}}}(\mu)$.

Our dual problem $\psi^{N_{\text{pr}}} \in X$ satisfies

$$a(v, \psi^{N_{\text{pr}}}(\mu); \mu) = p(u_{N_{\text{pr}}}(\mu) + u, v; \mu), \forall v \in X. \quad (33)$$

We then define our dual reduced-basis nested approximation spaces as $W_{N_{\text{du}}}^{\text{du}} \equiv \text{span}\{\psi^{N_{\text{pr}, \text{max}}}(\mu_n^{\text{du}}), 1 \leq n \leq N_{\text{du}}\} \equiv \text{span}\{\zeta_n^{\text{du}}, 1 \leq n \leq N_{\text{du}}\}$, $1 \leq N_{\text{du}} \leq N_{\text{du}, \text{max}}$, where our dual approximation, $\psi_{N_{\text{du}}}^{N_{\text{pr}}} \in W_{N_{\text{du}}}^{\text{du}}$, satisfies

$$a(v, \psi_{N_{\text{du}}}^{N_{\text{pr}}}(\mu); \mu) = p(2u_{N_{\text{pr}}}(\mu), v; \mu), \forall v \in W_{N_{\text{du}}}^{\text{du}} \quad (34)$$

and the dual residual is

$$r_{N_{\text{pr}}, N_{\text{du}}}^{\text{du}}(v; \mu) = p(2u_{N_{\text{pr}}}(\mu), v; \mu) - a(v, \psi_{N_{\text{du}}}^{N_{\text{pr}}}, v; \mu), \forall v \in X. \quad (35)$$

We consider our quadratic output

$$s_2(\mu) = p(u(\mu), u(\mu); \mu) \quad (36)$$

where $p(u(\mu), u(\mu); \mu)$ can be represented in the parametrized form as in (15). Our reduced-basis output approximation $s_{2, N}(\mu)$ is defined as

$$s_{2, N}(\mu) \equiv p(u_N(\mu), u_N(\mu)) + r_{N_{\text{pr}}}^{\text{pr}}(\psi_{N_{\text{du}}}^{N_{\text{pr}}}(\mu); \mu). \quad (37)$$

We can then prove

$$s_2(\mu) - s_{2, N}(\mu) = a(u - u_{N_{\text{pr}}}, \psi^{N_{\text{pr}}} - \psi_{N_{\text{du}}}^{N_{\text{pr}}}; \mu), \forall \mu \in \mathcal{D}, \quad (38)$$

which is the usual ‘‘quadratic’’ result [11].

B. Offline/Online approach

Even though $N_{\text{pr}}, N_{\text{du}}$ may be small, the elements of $W_{N_{\text{pr}}}^{\text{pr}}$ and $W_{N_{\text{du}}}^{\text{du}}$ are in some sense ‘‘large’’: for example $\zeta_n^{\text{pr}} \equiv u(\mu_n^{\text{pr}})$ will be represented in terms of $\mathcal{N} \gg N_{\text{pr}}$ truth finite element basis functions. To eliminate the \mathcal{N} -dependence, we employ the offline/online computational strategy.

To begin, we expand our reduced-basis approximation as

$$u_{N_{\text{pr}}}(\mu) = \sum_{j=1}^{N_{\text{pr}}} u_{N_{\text{pr}j}}(\mu) \zeta_j \quad (39)$$

$$\psi_{N_{\text{du}}}^{N_{\text{pr}}}(\mu) = \sum_{j=1}^{N_{\text{du}}} \psi_{N_{\text{du}j}}^{N_{\text{pr}}}(\mu) \zeta_j^{\text{du}} \quad (40)$$

Follows from (37) that the reduced-basis output can be expressed as

$$\begin{aligned} s_{2,N}(\mu) &= \sum_{j=1}^{N_{\text{pr}}} \sum_{j'=1}^{N_{\text{pr}}} \sum_{q=1}^{Q_p} u_{N_{\text{pr}j}}(\mu) u_{N_{\text{pr}j'}}(\mu) \Theta_p^q(\mu) p^q(\zeta_j^{\text{pr}}, \zeta_{j'}^{\text{pr}}) \\ &+ \sum_{j=1}^{N_{\text{du}}} \sum_{q=1}^{Q_f} \psi_{N_{\text{du}j}}(\mu) \Theta_f^q(\mu) f^q(\zeta_j^{\text{du}}) \\ &- \sum_{j=1}^{N_{\text{pr}}} \sum_{j'=1}^{N_{\text{du}}} \sum_{q=1}^{Q_a} u_{N_{\text{pr}j}}(\mu) \psi_{N_{\text{du}j'}}(\mu) \Theta_a^q(\mu) a^q(\zeta_j^{\text{pr}}, \zeta_{j'}^{\text{du}}) \end{aligned} \quad (41)$$

where the coefficients $u_{N_{\text{pr}j}}, 1 \leq j \leq N_{\text{pr}}$ and $\psi_{N_{\text{du}j}}, 1 \leq j \leq N_{\text{du}}$ satisfy the $N_{\text{pr}} \times N_{\text{pr}}$ and $N_{\text{du}} \times N_{\text{du}}$ linear algebraic systems

$$\sum_{j=1}^{N_{\text{pr}}} \left\{ \sum_{q=1}^{Q_a} \Theta_a^q(\mu) a^q(\zeta_j^{\text{pr}}, \zeta_i^{\text{pr}}) \right\} u_{N_{\text{pr}j}}(\mu) = \sum_{q=1}^{Q_f} \Theta_f^q(\mu) f^q(\zeta_i^{\text{pr}}), \quad 1 \leq i \leq N_{\text{pr}}, \quad (42)$$

and

$$\begin{aligned} \sum_{j=1}^{N_{\text{du}}} \left\{ \sum_{q=1}^{Q_a} \Theta_a^q(\mu) a^q(\zeta_i^{\text{du}}, \zeta_j^{\text{du}}) \right\} \psi_{N_{\text{du}j}}^{N_{\text{pr}}}(\mu) = \\ 2 \sum_{j=1}^{N_{\text{pr}}} \left\{ u_{N_{\text{pr}j}}(\mu) \sum_{q=1}^{Q_p} \Theta_p^q(\mu) p^q(\zeta_j^{\text{pr}}, \zeta_i^{\text{du}}) \right\}, \\ 1 \leq i \leq N_{\text{du}}. \end{aligned}$$

The offline/online decomposition is now clear. For simplicity, below we assume that $N_{\text{pr}} = N_{\text{du}} = N$.

In the offline stage – performed once – we first solve for the $\zeta_i^{\text{pr}}, \zeta_i^{\text{du}}, 1 \leq i \leq N$; we then form and store $f^q(\zeta_i^{\text{pr}}), f^q(\zeta_i^{\text{du}}), 1 \leq i \leq N, 1 \leq q \leq Q_f$; and $a^q(\zeta_i^{\text{pr}}, \zeta_j^{\text{pr}}), a^q(\zeta_i^{\text{du}}, \zeta_j^{\text{du}}), a^q(\zeta_i^{\text{pr}}, \zeta_j^{\text{du}}), 1 \leq i, j \leq N, 1 \leq q \leq Q_a$; and finally $Q_p(\zeta_i^{\text{pr}}, \zeta_j^{\text{pr}}), Q_p(\zeta_i^{\text{pr}}, \zeta_j^{\text{du}}), 1 \leq i, j \leq N, 1 \leq q \leq Q_p$. Note all the quantities computed in the offline stage are independent of the parameter μ . In the online stage – perform many times, for each new μ – we first form and invert the $N \times N$ matrix $\sum_{q=1}^{Q_a} \Theta_a^q(\mu) a^q(\zeta_i^{\text{du}}, \zeta_j^{\text{du}})$, solve for $u_{Nj}(\mu)$, and then form

TABLE I

REDUCED-BASIS APPROXIMATION CONVERGENCE

N	$\mathbf{E}_{1,N}$	$\mathcal{E}_{1,N}$	$\bar{\eta}_{1,N}^s$
5	1.65E-02	2.46E+00	96.4
10	2.23E-03	5.21E-02	48.6
15	3.89E-05	6.93E-04	41.6
20	5.13E-06	1.28E-04	43.5

N	$\mathbf{E}_{2,N}$	$\mathcal{E}_{2,N}$	$\bar{\eta}_{2,N}^s$
5	1.60E+00	1.07E+03	5915.2
10	2.91E-01	2.56E+01	1509.3
15	9.42E-04	5.21E-02	1218.4
20	3.53E-04	2.57E-02	770.1
25	1.50E-04	6.35E-03	538.5
30	9.39E-06	8.95E-04	443.7
35	4.57E-06	4.55E-04	520.5
40	8.99E-07	1.40E-04	589.4

and invert the $N \times N$ matrix $\sum_{q=1}^{Q_a} \Theta_a^q(\mu) a^q(\zeta_i^{\text{du}}, \zeta_j^{\text{du}})$, and then form $\sum_{q=1}^{Q_p} \Theta_p^q(\mu) p^q(\zeta_j^{\text{pr}}, \zeta_i^{\text{du}})$, which together will give us $\psi_{Nj}(\mu)$. We then perform the summation (41) – this yields $s_N(\mu)$. The operation counts for the online stage is $O((Q_p + Q_a)N^2)$ and $O(N^3)$, respectively, to form and invert the necessary matrices; and $O((Q_p + Q_a)N^2) + O(Q_f N)$ to evaluate the output. The essential point is the the online complexity is independence of \mathcal{N} . We expect significant computational savings since $N \ll \mathcal{N}$.

C. Numerical results

We present in Table I the convergence of our outputs. We present the results in term of $N = N_{\text{pr}} = N_{\text{du}}$. The error $\mathbf{E}_{2,N}$ is the maximum of the relative error, $|s_2(\mu) - s_{2,N}^1(\mu)| / |s_2^1(\mu)|$, over a random parameter test sample $\Xi_{\text{test}} \in \mathcal{D}$, of size $n_{\text{test}} = 1089$, where $s_1(\mu)$ and $s_2(\mu)$ are defined by (23). We observe very rapid convergence with N .

IV. A POSTERIORI ERROR ESTIMATION

A. Error estimation

We now assume that we are given $g_*^K(\mu)$ and $\tau_*^K(\mu)$, two positive functions which will be defined in the next section.

We now define our output error bound as

$$\begin{aligned} \Delta_N^{s_2}(\mu) &= \left(\frac{\tau_*^K(\mu)}{g_*^K(\mu)} \right)^2 \|r_{N_{\text{pr}}}^{\text{pr}}(\cdot, \mu)\|_{X'}^2 \\ &+ \frac{1}{\beta(\bar{\mu}) g_*^K(\mu)} \|r_{N_{\text{pr}}, N_{\text{du}}}^{\text{du}}(\cdot; \mu)\|_{X'} \|r_{N_{\text{pr}}}^{\text{pr}}(\cdot; \mu)\|_{X'}, \end{aligned} \quad (43)$$

where $\beta(\bar{\mu})$ is defined in (29).

It can be shown that

$$|s(\mu) - s_N(\mu)| \leq \Delta_N^s(\mu), \forall \mu \in \mathcal{D}. \quad (44)$$

TABLE II

COMPUTATIONAL COST TO EVALUATE $s_{N,2}$, $\Delta_N^{s_2}$, AND $s_2^{N_t}$ AS A FUNCTION OF N ($N = N_{\text{pr}} = N_{\text{du}}$); THE RESULTS ARE NORMALIZED WITH RESPECT TO THE TIME TO CALCULATE s_N FOR $N = 5$.

N	Online Time		Time $s_2^{N_t}$
	$s_{N,2}$	$\Delta_N^{s_2}$	
5	1.00	52.31	
10	1.20	53.81	
15	1.45	55.23	
20	1.98	57.01	
25	2.25	59.23	3900
30	2.71	61.81	
35	3.52	64.71	
40	4.44	67.87	

B. Construction of $g_*^K(\mu)$ and $\tau_*^K(\mu)$

We turn to the development of our functions $g_*^K(\mu)$ and $\tau_*^K(\mu)$, which was used in our error estimation.

1) *Construction of $g_*^K(\mu)$* : We define local natural-norm inf-sup and continuity parameters as

$$\beta_{\bar{\mu}}(\mu) \equiv \inf_{w \in X} \sup_{v \in X} \frac{a(w, v; \mu)}{\|w\|_{\bar{\mu}} \|v\|_X} \equiv \inf_{w \in X} \frac{\|T^\mu w\|_X}{\|T^{\bar{\mu}} w\|_X} \quad (45)$$

$$\gamma_{\bar{\mu}}(\mu) \equiv \sup_{w \in X} \sup_{v \in X} \frac{a(w, v; \mu)}{\|w\|_{\bar{\mu}} \|v\|_X} \equiv \sup_{w \in X} \frac{\|T^\mu w\|_X}{\|T^{\bar{\mu}} w\|_X}, \quad (46)$$

respectively. It is clear the for $\mu = \bar{\mu}$, $\beta_{\bar{\mu}} = \gamma_{\bar{\mu}} = 1$. We can also related the new norm with the original norm by proving that

$$\beta(\bar{\mu})\beta_{\bar{\mu}}(\mu) \leq \beta(\mu) \leq \gamma(\bar{\mu})\beta_{\bar{\mu}}(\mu). \quad (47)$$

We further define

$$\bar{\beta}_{\bar{\mu}}(\mu) \equiv \inf_{w \in X} \frac{(T^\mu w, T^{\bar{\mu}} w)_X}{\|w\|_{\bar{\mu}}^2}. \quad (48)$$

By Cauchy-Schwarz inequality, we can prove that

$$\bar{\beta}_{\bar{\mu}}(\mu) \leq \beta_{\bar{\mu}}(\mu). \quad (49)$$

or $\bar{\beta}_{\bar{\mu}}$ is an approximation of $\beta_{\bar{\mu}}$.

It can be further shown that $|\beta_{\bar{\mu}} - \bar{\beta}_{\bar{\mu}}(\mu)| \sim |\mu - \bar{\mu}|^2$, $\mu \rightarrow \bar{\mu}$, where $|\cdot|$ refers to the usual Euclidean norm. The result is that $\bar{\beta}_{\bar{\mu}}(\mu)$ is a second-order accurate approximation to $\beta_{\bar{\mu}}(\mu)$.

We next introduce a set of parameter points $\mathcal{V}^K \equiv \{\bar{\mu}_1 \in \mathcal{D}, \bar{\mu}_2 \in \mathcal{D}, \dots, \bar{\mu}_K \in \mathcal{D}\}$ an an associated ‘‘indicator’’ function $\bar{\mu}_*^K : \mathcal{D} \rightarrow \mathcal{V}^K$ which maps any given $\mu \in \mathcal{D}$ to the appropriate local approximation. Our global piecewise natural norm inf-sup parameter is then

$$\beta_*^K(\mu) = \beta_{\bar{\mu}_*^K(\mu)}(\mu). \quad (50)$$

We now turn to the construction of this lower bound approximation.

We begin with a local lower bound. For given $\bar{\mu} \in \mathcal{D}$, we

introduce the function $g_{\bar{\mu}} : \mathcal{D} \rightarrow \mathbb{R}$

$$g_{\bar{\mu}}(\mu) = \max_{\kappa \in \mathbb{R}^P} \left\{ 1 + \sum_{p=1}^P \min[\kappa_p(\mu_p - \bar{\mu}_p)\lambda_{\bar{\mu}, \max}^p, \kappa_p(\mu_p - \bar{\mu}_p)\lambda_{\bar{\mu}, \min}^p] \right. \\ \left. + \sum_{q=1}^Q \min \left[\left(\Theta^q(\mu) - \Theta^q(\bar{\mu}) - \sum_{p'=1}^P \frac{\partial \Theta^q}{\partial \mu_{p'}}(\bar{\mu}) \kappa_{p'}(\mu_{p'} - \bar{\mu}_{p'}) \right) \xi_{\bar{\mu}, \max}^q, \right. \right. \\ \left. \left. \left(\Theta^q(\mu) - \Theta^q(\bar{\mu}) - \sum_{p'=1}^P \frac{\partial \Theta^q}{\partial \mu_{p'}}(\bar{\mu}) \kappa_{p'}(\mu_{p'} - \bar{\mu}_{p'}) \right) \xi_{\bar{\mu}, \min}^q \right] \right\} \quad (51)$$

where, for $p = 1, \dots, P$,

$$\lambda_{\bar{\mu}, \min(\max)}^p = \min_{w \in X} (\max_{w \in X}) \frac{\sum_{q=1}^Q \frac{\partial \Theta^q}{\partial \mu_p}(\bar{\mu}) a^q(w, T^{\bar{\mu}} w)}{\|w\|_{\bar{\mu}}^2} \quad (52)$$

and, for $q = 1, \dots, Q$,

$$\xi_{\bar{\mu}, \min(\max)}^p = \min_{w \in X} (\max_{w \in X}) \frac{a^q(w, T^{\bar{\mu}} w)}{\|w\|_{\bar{\mu}}^2}. \quad (53)$$

We can then prove, for given $\bar{\mu} \in \mathcal{D}$, $g_{\bar{\mu}}(\mu) \leq \bar{\beta}_{\bar{\mu}}(\mu)$, $\forall \mu \in \mathcal{D}$. That makes $g_{\bar{\mu}}(\mu)$ a lower bound approximation of $\bar{\beta}_{\bar{\mu}}(\mu)$.

To compute $g_{\bar{\mu}}(\mu)$, we note that we can write it in the form

$$g_{\bar{\mu}}(\mu) = 1 + \max_{\kappa \in \mathbb{R}^P} \sum_{m=1}^{P+Q} \min[F_m(\kappa), G_m(\kappa)] \quad (54)$$

where the F_m, G_m , $1 \leq m \leq P+Q$ are affine functions of κ . The sum (54) is essentially a Linear Program.

We can further enhance the sharpness of our lower bound for $\bar{\beta}_{\bar{\mu}}(\mu)$ by optimally locally align a parameter coordinate with the largest gradients in $\bar{\beta}_{\bar{\mu}}$ [13].

Our global lower bound, $g_*^K : \mathcal{D} \rightarrow \mathbb{R}$, is then given by

$$g_*^K(\mu) = \max_{\bar{\mu} \in \mathcal{V}^K} g_{\bar{\mu}}(\mu), \quad (55)$$

we further define $g_{*, \min}^K \equiv \min_{\mu \in \mathcal{D}} g_*^K(\mu)$ and specify our indicator function $\bar{\mu}_*^K : \mathcal{D} \rightarrow \mathcal{V}^K$ as

$$\bar{\mu}_*^K(\mu) = \arg \max_{\bar{\mu} \in \mathcal{V}^K} g_{\bar{\mu}}(\mu), \quad (56)$$

in terms of which our lower bound may be expressed as

$$g_*^K(\mu) = g_{\bar{\mu}_*^K(\mu)}(\mu). \quad (57)$$

We can prove that, for any given set of points \mathcal{V}^K ,

$$g_*^K(\mu) \leq \beta_*^K(\mu), \forall \mu \in \mathcal{D}. \quad (58)$$

We finally propose a procedure to determine the set of parameter points \mathcal{V}^K so that our lower bound is of value. We first introduce a large parameter sample $\Xi_g \in \mathcal{D}$ of size $n^g \gg 1$. We next set $K = 1$ and select a tolerance $0 < g_{*, \text{tol}} < 1$; we then choose $\bar{\mu}_1$ which defines $g_*^1(\mu)$. We now proceed to calculate for $K = 1, \dots$

$$\bar{\mu}_{K+1} = \arg \max_{\mu \in \Xi_g} \min_{\mu' \in \Xi_g | g_*^K(\mu') \geq g_{*, \text{tol}}} |\mu - \mu'| \quad (59)$$

where the $|\cdot|$ norm can be chosen as the usual Euclidean norm, until

$$\min_{\mu' \in \Xi_g} g_*^K(\mu) \geq g_{*, \text{tol}}. \quad (60)$$

We note that the new proposed procedure above to both construct the offline data – set of parameter points \mathcal{V}^K and their associated data – and online evaluation can be done automatically.

2) *Construction of $\tau_*^K(\mu)$* : For each $\bar{\mu} \in \mathcal{D}$, we define

$$\bar{\tau}_{\bar{\mu}}^2(\mu) = \sup_{v \in X} \frac{p(v, v; \mu)}{\|T\bar{\mu}v\|_X^2}. \quad (61)$$

The upper bound of $\bar{\tau}_{\bar{\mu}}$ can be taken as

$$\tau_{\bar{\mu}}^2(\mu) = \sum_{q=1}^{Q_p} |\Theta_p^q(\mu)| \sup_{v \in X} \frac{p^q(v, v)}{\|T\bar{\mu}v\|_X^2}. \quad (62)$$

Our parameter $\tau_*^K : \mathcal{D} \rightarrow \mathbb{R}$ is then given by

$$\tau_*^K(\mu) = \tau_{\bar{\mu}_*^K}(\mu). \quad (63)$$

C. Offline/Online approach

We first demonstrate the offline/online decomposition for the term $\|r_{N_{\text{pr}}}^{\text{pr}}(\cdot, \mu)\|_{X'}$.

To begin, we note that from duality argument that

$$\|r_{N_{\text{pr}}}^{\text{pr}}(\cdot, \mu)\|_{X'} = \sup_{v \in X} \frac{r_{N_{\text{pr}}}^{\text{pr}}(v, \mu)}{\|v\|} = (\hat{e}(\mu), v), v)_X \quad (64)$$

where $\hat{e}(\mu) \in X$ satisfies

$$(\hat{e}(\mu), v), v)_X = r_{N_{\text{pr}}}^{\text{pr}}(v, \mu). \quad (65)$$

It follows from

$$\begin{aligned} r_{N_{\text{pr}}}^{\text{pr}}(v, \mu) &= \sum_{q=1}^{Q_f} \Theta_f^q(\mu) f^q(v) \\ &\quad - \sum_{q=1}^{Q_a} \sum_{n=1}^{N_{\text{pr}}} \Theta_a^q(\mu) u_{N_{\text{pr}}n} a^q(\zeta_n^{N_{\text{pr}}}, v), \end{aligned} \quad (66)$$

and linear superposition that

$$\hat{e}(\mu) = \sum_{q=1}^{Q_f} \Theta_f^q \mathcal{C}^q + \sum_{q=1}^{Q_a} \sum_{n=1}^{N_{\text{pr}}} \Theta_a^q u_{N_{\text{pr}}n} \mathcal{L}_n^q, \quad (67)$$

where $\mathcal{C}^q \in X, 1 \leq q \leq Q_f$ and $\mathcal{L}_n^q \in X, 1 \leq n \leq Q_a, 1 \leq n \leq N_{\text{pr}}$ satisfies the parameter-independence problems $(\mathcal{C}^q, v) = f^q(v), \forall v \in X$ and $(\mathcal{L}_n^q, v) = -a^q(\zeta_n^{\text{pr}}, v), \forall v \in X$, respectively. We then obtain

$$\begin{aligned} \|r_{N_{\text{pr}}}^{\text{pr}}(\cdot, \mu)\|_{X'}^2 &= \sum_{q=1}^{Q_f} \sum_{q'=1}^{Q_f} \Theta_f^q(\mu) \Theta_f^{q'}(\mu) (\mathcal{C}^q, \mathcal{C}^{q'})_X \\ &\quad + 2 \sum_{q=1}^{Q_f} \sum_{q'=1}^{Q_a} \sum_{n=1}^{N_{\text{pr}}} \Theta_f^q(\mu) \Theta_a^{q'}(\mu) u_{N_{\text{pr}}n} (\mathcal{C}^q, \mathcal{L}_n^{q'})_X \\ &\quad + \sum_{q=1}^{Q_a} \sum_{q'=1}^{Q_a} \sum_{n=1}^{N_{\text{pr}}} \sum_{n'=1}^{N_{\text{pr}}} \Theta_a^q(\mu) \Theta_a^{q'}(\mu) u_{N_{\text{pr}}n} u_{N_{\text{pr}}n'} (\mathcal{L}_n^q, \mathcal{L}_{n'}^{q'})_X. \end{aligned} \quad (68)$$

Similarly, we can obtain

$$\begin{aligned} \|r_{N_{\text{pr}}, N_{\text{du}}}^{\text{du}}(\cdot; \mu)\|_{X'}^2 &= \\ &\sum_{q=1}^{Q_p} \sum_{q'=1}^{Q_p} \sum_{n=1}^{N_{\text{pr}}} \sum_{n'=1}^{N_{\text{pr}}} \Theta_p^q(\mu) \Theta_p^{q'}(\mu) u_{N_{\text{pr}}n}(\mu) u_{N_{\text{pr}}n'}(\mu) (\mathcal{Q}_n^q, \mathcal{Q}_{n'}^{q'})_X \\ &\quad + 2 \sum_{q=1}^{Q_p} \sum_{q'=1}^{Q_a} \sum_{n=1}^{N_{\text{pr}}} \sum_{n'=1}^{N_{\text{du}}} \Theta_p^q(\mu) \Theta_a^{q'}(\mu) u_{N_{\text{pr}}n}(\mu) \psi_{N_{\text{du}}n'}(\mu) (\mathcal{Q}_n^q, \mathcal{M}_{n'}^{q'})_X \\ &\quad + \sum_{q=1}^{Q_a} \sum_{q'=1}^{Q_a} \sum_{n=1}^{N_{\text{du}}} \sum_{n'=1}^{N_{\text{du}}} \Theta_a^q(\mu) \Theta_a^{q'}(\mu) u_{N_{\text{du}}n}(\mu) \psi_{N_{\text{du}}n'}(\mu) (\mathcal{M}_n^q, \mathcal{M}_{n'}^{q'})_X. \end{aligned} \quad (69)$$

where $\mathcal{Q}_n^q \in X, 1 \leq n \leq Q_p, 1 \leq n \leq N_{\text{pr}}$ and $\mathcal{M}_n^q \in X, 1 \leq n \leq Q_a, 1 \leq n \leq N_{\text{du}}$ satisfies the parameter-independence problems $(\mathcal{Q}_n^q, v) = p^q(2\zeta_n^{\text{pr}}, v), \forall v \in X$ and $(\mathcal{M}_n^q, v) = -a^q(\zeta_n^{\text{du}}, v), \forall v \in X$, respectively.

For the sake of simplicity below, we assume that $N = N_{\text{du}} = N_{\text{pr}}$. The offline-online decomposition is now identified. In the offline stage – performed once – we first solve for $\mathcal{C}^q, 1 \leq q \leq Q_f$ and $\mathcal{L}_n^q, 1 \leq q \leq Q_a, 1 \leq n \leq N$ and $\mathcal{Q}_n^q, 1 \leq q \leq Q_p, 1 \leq n \leq N$ and $\mathcal{M}_n^q, 1 \leq q \leq Q_a, 1 \leq n \leq N$; we then evaluate and store all the parameter-independence inner products $(\mathcal{C}^q, \mathcal{C}^q)_X, (\mathcal{C}^q, \mathcal{L}_n^{q'})_X, (\mathcal{L}_n^q, \mathcal{L}_{n'}^{q'})_X, (\mathcal{Q}_n^q, \mathcal{Q}_{n'}^{q'})_X, (\mathcal{Q}_n^q, \mathcal{M}_{n'}^{q'})_X, (\mathcal{M}_n^q, \mathcal{M}_{n'}^{q'})_X, 1 \leq n, n' \leq N, 1 \leq q, q' \leq Q_f, Q_a, Q_p$. In the online stage – performed many times, for any new value of μ – we simply evaluate $\|r_{N_{\text{pr}}}^{\text{pr}}(\cdot, \mu)\|_{X'}$ and $\|r_{N_{\text{pr}}, N_{\text{du}}}^{\text{du}}(\cdot; \mu)\|_{X'}$ in terms of $\Theta_f^q, \Theta_a^q, \Theta_p^q, u_{N_{\text{pr}}n}(\mu)$ and $\psi_{N_{\text{du}}n}(\mu)$ and the precomputed and stored $(\cdot, \cdot)_X$ inner products. The operation count for the online stage is $O((Q_a^2 + Q_p^2 + Q_a Q_p)N^2)$ – independent of \mathcal{N} – and commensurate with the online cost to evaluate $s_N(\mu)$.

D. Sampling procedure

Our error estimation procedures also allow us to construct good parameter samples $S_{N_{\text{pr}}}^{\text{pr}}, S_{N_{\text{du}}}^{\text{du}}$ (and hence spaces $W_{N_{\text{pr}}}^{\text{pr}}, W_{N_{\text{du}}}^{\text{du}}$). We only present the procedure to construct $S_{N_{\text{pr}}}^{\text{pr}}$ here, since $S_{N_{\text{du}}}^{\text{du}}$ can be constructed in a similar manner.

We first introduce a large parameter sample Ξ_{test} in \mathcal{D} of size $n^{\text{test}} \gg 1$. We then set $N = 1$ and choose μ_1^{pr} which defines the first basis ζ_1^{pr} . We now then proceed for $N = 1, \dots, N_{\text{pr}}$

$$\mu_{N+1}^{\text{pr}} = \arg \max_{\mu \in \Xi_{\text{test}}, \mu \notin S^{\text{pr}}} \frac{1}{\sqrt{\beta(\bar{\mu}) g_*^K(\mu)}} \|r_N^{\text{pr}}(\cdot; \mu)\|_{X'} \quad (70)$$

where $\beta(\bar{\mu})$ is defined in (29). The crucial point is that the terms that appear in the right hand side of (70) can be computed “online-inexpensively” and presented the true primal error $\|u(\mu) - u_N(\mu)\|_X$. This permit us perform a very exhaustive ($n^{\text{test}} \gg 1$) search for the best sample $S_N^{\text{pr}}, S_N^{\text{du}}$ and, hence, determine the smallest N for which we achieve the desired accuracy.

E. Numerical Results

We first apply algorithm (59) for the uniform grid Ξ_g over \mathcal{D} of size $n_g = 1089$; we satisfy the desired tolerance for $K = 11$ for the criteria $g_{*, \text{tol}} = 0.5$.

We present in Table I the convergence of our output. We present the results in term of $N = N_{\text{pr}} = N_{\text{du}}$. The error $E_{1,N}$ is the maximum of the relative error, $|s_1(\mu) - s_{1,N}^s(\mu)|/|s_1(\mu)|$, and the error bound $\mathcal{E}_{1,N}^s$ is the maximum of the relative error bound, $|\Delta_N^{s_1}(\mu)|/|s_1(\mu)|$, over a uniform parameter test sample $\Xi_{\text{test}} \in \mathcal{D}$, of size $n_{\text{test}} = 1089$; the effectivity $\bar{\eta}_N^s$ is the average of the effectivity, $\eta_N^s(\mu) = \Delta_N^s(\mu)/|s(\mu) - s_N(\mu)|$, over the parameter test sample Ξ_{test} . We observe that the effectivities of the linear output $s_1(\mu)$ are good, but the effectivities of the quadratic output $s_2(\mu)$ are quite high. The reason is maybe due to the large ratio $\tau_*^K(\mu)/g_*^K(\mu)$ (which is order of ten) which appears in our error estimation.

We also present in Table II the online reduced-basis computational cost to evaluate $s_{N,2}(\mu)$ and its error bound $\Delta_N^{s_2}$ to the finite element cost to evaluate $s_2^{N_t}$ for any given μ . Although we expect that the online times to calculate $s_{N,2}$ and $\Delta_N^{s_2}$ should be commensurate with each other, we observe that the $\Delta_N^{s_2}$ computational time is much more than that of $s_{N,2}$. The reason is that the online time to calculate $\Delta_N^{s_2}$ is ‘‘polluted’’ by a poor LP solver for computing the $g_*^K(\mu)$ (55); 70% of the time is due to the LP.

V. APPLICATIONS

To demonstrate the advantage of our method, we apply our results to some simple fracture mechanics problems. We only focus on using our technique to predict failure for simple brittle material in this paper, but other applications include fatigue crack growth, and prediction crack instability based on ‘‘R’’ curves [6].

The theory of fracture of brittle materials is developed by Griffith, who proposed his well-known Griffith’s theory. Griffith formulated the concept that a crack in a component will propagate if the total energy of the system is lowered with crack propagation. That is, if the change in elastic strain energy due to crack extension is larger than the energy required to create new crack surfaces, crack propagation will occur.

Previously, we have constructed the reduced-basis approximation to estimate SIFs for the two-layers plate problem. In short, the reduced-basis approximation can be estimate SIFs in real-time for an arbitrary parameter $\mu \in \mathcal{D}$, where $\mathcal{D} = [2.0, 4.0] \times [0.1, 10.0]$. For a given set of ‘‘inputs’’ $(\tilde{d}, \tilde{t}, \tilde{E}_1, \tilde{E}_2)$, we can estimate the ERR as the output $\tilde{G} \equiv s(\mu)$. Moreover, if we define

$$\hat{s}(\mu) = \sqrt{s(\mu)}, \quad (71)$$

then the reduced-basis approximation $\hat{s}_N(\mu)$ and its error estimation $\Delta_N^{\hat{s}}(\mu)$ are given by

$$\begin{aligned} \hat{s}_N(\mu) &= \frac{1}{2} \left\{ \sqrt{s_N(\mu) - \Delta_N^s(\mu)} + \sqrt{s_N(\mu) + \Delta_N^s(\mu)} \right\} \\ \Delta_N^{\hat{s}}(\mu) &= \frac{1}{2} \left\{ \sqrt{s_N(\mu) + \Delta_N^s(\mu)} - \sqrt{s_N(\mu) - \Delta_N^s(\mu)} \right\}. \end{aligned} \quad (72)$$

We consider an uncertainty parameter region $[\tilde{d}, \tilde{t}, \tilde{E}_2] \in \tilde{\mathcal{D}}^u$, where $\tilde{\mathcal{D}}^u \equiv [2.8, 3.2](\text{mm}) \times [0.8, 1.2](\text{mm}) \times [50, 500](\text{GPa})$ where \tilde{E}_2 is the Young’s modulus of the coating material. We use the material Silicate SiO₂ S100a, with material properties are $\tilde{K}_{IC} = 0.73\text{MPa}\sqrt{\text{m}}$ and

$\tilde{E}_1 = 79.23\text{GPa}$ [4], for the simulation. Physically, the Young’s modulus \tilde{E}_2 of the coating region changes due to environmental conditions [4]. We are interested in finding the maximum applied traction $\tilde{\sigma}_0$ so that the condition $\tilde{K}_{\text{worstcase}} = 0.5\tilde{K}_{IC}$ is still satisfied. This condition is equivalent to the condition that the crack will not propagate with safety factor 0.5 according to Griffith’s theory.

From (10), we can write

$$\sigma_0 \leq \frac{0.5K_{IC}}{\sqrt{\tilde{t}} \sqrt{G\left(\frac{\tilde{d}}{\tilde{t}}, \frac{\tilde{E}_2}{\tilde{E}_1}\right)}} = \mathcal{F}(\tilde{d}, \tilde{t}, \tilde{E}_2), \quad (73)$$

which gives

$$\sigma_{0,\text{max}} = \min_{(\tilde{d}, \tilde{t}, \tilde{E}_2) \in \tilde{\mathcal{D}}^u} \mathcal{F}(\tilde{d}, \tilde{t}, \tilde{E}_2). \quad (74)$$

Denote

$$\mathcal{F}_N(\tilde{d}, \tilde{t}, \tilde{E}_2) = \frac{0.5K_{IC}}{\sqrt{\tilde{t}} \left[\hat{s}_N\left(\frac{\tilde{d}}{\tilde{t}}, \frac{\tilde{E}_2}{\tilde{E}_1}\right) + \Delta_N^{\hat{s}}\left(\frac{\tilde{d}}{\tilde{t}}, \frac{\tilde{E}_2}{\tilde{E}_1}\right) \right]} \quad (75)$$

where \hat{s}_N and $\Delta_N^{\hat{s}}$ are defined in (72), then our approximation optimization is

$$\sigma_{0,\text{max},N} = \min_{(\tilde{d}, \tilde{t}, \tilde{E}_2) \in \tilde{\mathcal{D}}^u} \mathcal{F}_N(\tilde{d}, \tilde{t}, \tilde{E}_2). \quad (76)$$

By solving the above optimization problem, the ‘‘feasibility/safety’’ condition is ensured thanks to our *a posteriori* error estimation. We note that the ERR for our problem is not monotonically increasing with \tilde{d} , since it is affected by the Dirichlet boundary conditions on Γ_R , hence a search is necessary. We will apply a ‘‘brute-force’’ method to search for the minimum value of $\mathcal{F}_N(\tilde{d}, \tilde{t}, \tilde{E}_2)$ for a very fine grid points, even though more general optimization algorithms are applicable. We consider 8000 sample points and obtain the maximum applied traction force $\tilde{\sigma}_{0,\text{max},N} = 7.6266\text{N/m}$ where the parameter is $[\tilde{d}, \tilde{t}, \tilde{E}_2] = [2.8(\text{mm}), 1.2(\text{mm}), 500(\text{GPa})]$. This critical point is clearly not obvious. The simulation takes less than 5 minutes in total, which is about 40 milliseconds for each parameter test point on a P4 1.5GHz computer. This demonstrates that in many-query applications, our method will work very efficiently.

VI. CONCLUSIONS

In this study, we show that, with the use of our reduced-basis approximation, fracture parameters - SIF and ERR values - can be calculated rapidly yet rigorously by certified error estimation. This offers a new, very promising approach for many failure analysis applications that require both real-time and/or many-query evaluations.

ACKNOWLEDGMENT

We would like to thank Professor David M. Parks of MIT, Professor David Clarke and Professor Tony Evans of USC B for many helpful recommendations. This work was supported by DARPA and AFOSR under Grant F49620-03-1-0356 and the Singapore-MIT Alliance.

REFERENCES

- [1] I. Babuska and J. M. Melenk. The partition of unity method. *International Journal for Numerical Methods in Engineering*, pages 727–758, 1997.
- [2] Roshdy S. Barsoum. On the use of isoparametric finite elements in linear fracture mechanics. *International Journal of Numerical Methods in Engineering*, pages 25–37, 1976.
- [3] C. Daux, N. Moës, J. Dolbow, N. Sukumar, and T. Belytschko. A finite element method for crack growth without remeshing. *International Journal for Numerical Methods in Engineering*, pages 131–150, 1999.
- [4] S. W. Freiman, T. L. Baker, and Jr J. B. Wachtman. *A Computerized Fracture Mechanics Database for Oxide Glasses*. NBS Technical Note 1212 (National Bureau of Standards), 1985.
- [5] R. D. Henshell and K. G. Shaw. Crack tip finite elements are unnecessary. *International Journal of Numerical Methods in Engineering*, pages 495–507, 1975.
- [6] John W. Hutchinson. *Nonlinear Fracture Mechanics*. Monograph, Department of Solid Mechanics, Technical University, Denmark, 1979.
- [7] Jeong-Ho Kim and Glaucio H. Paulino. Finite element evaluation of mixed mode stress intensity factors in functionally graded materials. *International Journal for Numerical Methods in Engineering*, pages 1903–1935, 2002.
- [8] F. Z. Li, C. F. Shih, and A. Needleman. A comparison of methods for calculating energy release rates. *Engineering Fracture Mechanics*, pages 405–421, 1985.
- [9] Y. Murakami. *Stress Intensity Factors Handbook*. Elsevier, 2001.
- [10] D. M. Parks. A stiffness derivative finite element technique for determination of crack tip stress intensity factors. *International Journal of Fracture*, 10(4):487–502, 1977.
- [11] N. A. Pierce and M. B. Giles. Adjoint recovery of superconvergent functionals from pde approximations. *SIAM Review*, (2):247–264, 2000.
- [12] G. Strang and G. J. Fix. *An analysis of the Finite Element Method*. Prentice-Hall, 1973.
- [13] S. Sugata, K. Veroy, D. B. P. Huynh, S. Deparis, N. C. Nguyen, and A. T. Patera. Uncertainty quantification for reduced-basis approximations: A *Posteriori* error estimators. *JCP Special Volume on Uncertainty Quantification*, (submitted), 2005.